ORIGINAL PAPER: FUNDAMENTALS OF SOL–GEL AND HYBRID MATERIALS PROCESSING

Molecular dynamics and partition of impurity molecules in silicates during sol–gel processes: spin probe EPR study

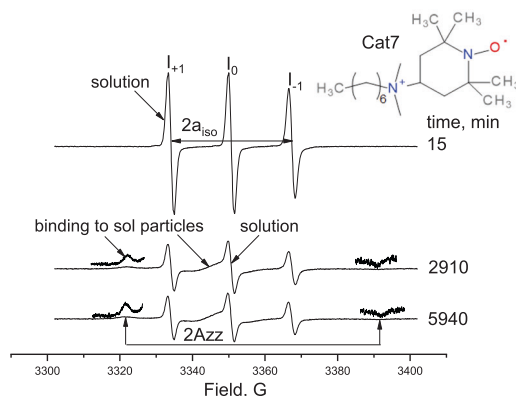I. V. Ionova[1] · A. A. Medvedeva[1] · A. V. Koshkin[1] · V. A. Livshits[1]

Abstract

The molecular dynamics and partition of nitroxide spin probes in the tetrakis(2-hydroxyethyl) orthosilicate (THEOS)/ethylene glycol/water system during its transformation from a liquid solution into a sol and gel structures were studied depending on the processing time and the pH of the medium. In acidic (pH 3.5) and neutral (pH 6.8) media, an increase in the effective rotation correlation time (τ_{eff}) of positively charged probes (Cat 7 and Cat 14) in the liquid phase of the sol–gel system and a subsequent decrease in τ_{eff} was found, with the growth and a decay times of τ_{eff} decreasing with an increase in pH. The values of τ_{eff} are due to the "dynamic exchange" of probes between the solution and the surface of colloidal particles formed in the sol–gel process. The decrease in τ_{eff} is apparently due to a slowdown in the exchange of probes between the solution and the surface of the particles due to a decrease in the surface during the enlargement of particles, as well as to the formation of a gel. These changes are accompanied by a decrease in the concentration of probes in the solution and the appearance of strongly immobilized EPR signals (SIS), apparently from probes that are bound in the bulk of sol and gel particles and do not exchange with the solution. The sizes of sol particles, determined from the parameters of the SIS shape, increase with the duration of incubation in the range of several nm.

Graphical abstract

Spin probe EPR spectra in tetrakis(2-hydroxyethyl) orthosilicate/ethylene glycol/water system at different processing times.

✉ V. A. Livshits
vlivshi@mail.ru

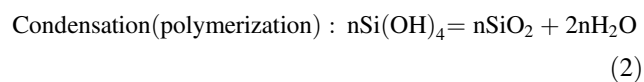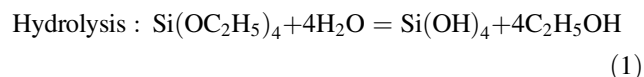1 Photochemistry Centre RAS, FSRC "Crystallography and Photonics" RAS, Novatorov 7a, 119421 Moscow, Russia

Highlights

- The molecular dynamics and partition of the positively charged nitroxide spin probes in the tetrakis(2-hydroxyethyl) orthosilicate/ ethylene glycol/water system during its processing from liquid solution into sol/gel were studied depending on the processing time and pH.
- In the liquid phase, an increase in the effective rotational correlation time (τ_{eff}) of the probes and subsequent decrease in τ_{eff} occur. These changes are due to the dynamic exchange of probes between the solution and surface of the colloidal particles formed.
- The above changes are accompanied by appearance of probes immobilized in the bulk of particles and not exchanging with the solution. The sizes of sol particles increase in the range of several nm during the processing time.

1 Introduction

Materials based on sol–gel processes using silicates are widely used as matrixes for the incorporation of functional molecules of various natures into them (fluorophores, photochromes, proteins, etc.). A large number of works have been devoted to the study of sol–gel processes based on TEOS ($Si(OC_2H_5)_4$ and TMOS ($Si(OCH_3)_4$ silicates using magnetic resonance and optical spectroscopy methods [1–13]. TEOS and TMOS molecules are initial (or intermediate) compounds that react with the formation of Si-O-Si bonds. The reactions of hydrolysis and polymerization lead to an increase in viscosity until the solution stops flowing. The sol–gel transition is irreversible; instead of a single-phase sol solution, a two-phase gel–liquid system arises that initially consists of amorphous particles of various sizes (5–12 nm or less) with gaps filled with a liquid phase. At the stage of gel formation, the gaps are compressed to form pores and the liquid phase fills these pores. After the formation of gels, they usually undergo an aging process, in which gels close, and a small amount of the liquid phase is lost. The condensation reactions continue, increasing the number of crosslinks in three-dimensional network. During the drying process, part of the liquid phase is removed, and the volume of the solvent is reduced [2, 5].

The sol–gel process is usually divided into the following stages: sol formation, gelation, aging, drying, and densification. The total reactions involving TEOS and TMOS, leading to the formation of gels, can be described by Eqs. (1) and (2):

$$\text{Hydrolysis}: Si(OC_2H_5)_4 + 4H_2O = Si(OH)_4 + 4C_2H_5OH \tag{1}$$

$$\text{Condensation(polymerization)}: nSi(OH)_4 = nSiO_2 + 2nH_2O \tag{2}$$

When functional impurity molecules are used as probes for studying a sol–gel process or materials for photonics, the most important problem is to establish the localization of probes in a heterogeneous sol–gel matrix, since localization determines the environment and spectral properties of these molecules. At present, it is generally accepted that there are four main types of environment for impurity molecules in a sol–gel matrix: the interior of a pore (often filled with a solution), the interface between the liquid and the pore wall, the pore wall itself, and the region in which the distance between opposite pore walls is approximately the same as the size of the molecule itself [5].

In this work, we investigated the partition and dynamics of impurity molecules—spin probes, introduced into a silicate solution and the change in these parameters during the transition of the solution into a heterogeneous sol–gel system depending on the processing time after its preparation at different pH of the medium. Tetrakis(2-hydroxyethyl) orthosilicate (THEOS) [9] was used as the starting silicate, in which, unlike methoxy and ethoxy groups, 2-hydroxyethyl, $Si(OC_2H_5OH)_4$, is used. The advantage of this precursor over TEOS and TMOS is good water solubility and full compatibility with biopolymers. THEOS is hydrolyzed in an aqueous solution with the release of ethylene glycol (EG), the formation of silanol groups Si-OH and silicic acid $Si(OH)_4$ [9, 10].

Earlier, a number of studies of TEOS-based sol–gel systems were carried out by EPR spectroscopy using nitroxyl radicals [4, 6, 8] and transition metal ions [12, 13] as spin probes; however, the kinetics of transformations of the sol–gel system at its initial stages and its dependence on the pH of the medium in these works were not studied in detail. In refs. [14–16], the adsorption and molecular dynamics of spin probes on silica gel microspheres, as well as the formation of guest-host complexes of spin probes with cyclodextrins bound to silica gel particles from the gas phase, were studied.

In this work, we studied the initial stages of the THEOS-based sol–gel process, up to the formation of a gel using nitroxide spin probes as impurity functional molecules, and the dependence of the kinetics of this process on the pH of the medium. We used nitroxide probes of various structures: Cat 7 and Cat 14 radicals with a positive charge on the quaternary nitrogen atom and different lengths of the alkyl group (heptyl and myristoyl, respectively) linked to the quaternary nitrogen atom, as well as a neutral K6 probe containing an aromatic indole nucleus.

2 Experimental

2.1 Materials

A spin-labeled analog of indole with a piperidine moiety (radical K6, Fig. 1) was synthesized by PhD A.B. Shapiro et al. Radicals Cat 7 and Cat 14 (Fig. 2) were kindly provided by Dr Sc. G.B. Khomutov (Moscow State University); EG is from Aldrich. THEOS (Fig. 3) was synthesized by us according to the method described in ref. [11].

2.2 Preparation of samples for EPR spectroscopy

A 10^{-2} M spin probe solution in EG was mixed with THEOS, and bidistilled water was added to the mixture. After vigorous stirring, the sample was transferred to a glass capillary (Brand, FRG, inner diameter 1.2 mm) and EPR spectra were recorded. The concentration of the spin probe
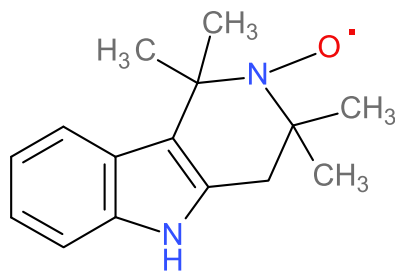

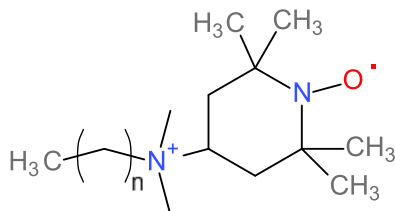Fig. 1 Structure of spin-labeled indole (K6)

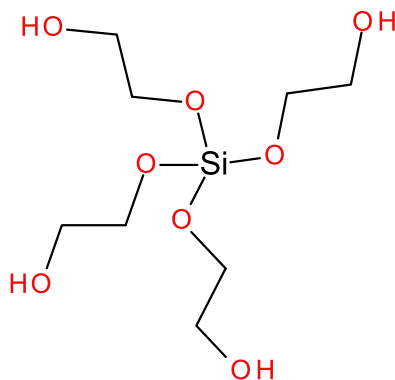Fig. 2 Structures of Cat 7 ($n = 6$) and Cat 14 ($n = 13$)

Fig. 3 Structure of THEOS

in the sample was 3×10^{-4} M, the content of THEOS: 0.73 M, water: 80% v/v, EG: 3% v/v.

2.3 Measurement and analysis of EPR spectra

EPR spectra were recorded on a Brucker-ER-200 instrument with a standard E102 rectangular cavity under thermostating conditions at a microwave frequency of 9.5 GHz in a magnetic field of 3356 gauss and a magnetic modulation frequency of 100 kHz. The values of the incident microwave power and modulation amplitude excluded the distortion of the EPR spectra. The correlation times of the probe rotation in the region of fast rotations in the isotropic rotation approximation were determined from the EPR spectra using the relation [17, 18]:

$$\tau_{\text{eff}} = 6.65 \cdot 10^{-10} \cdot \Delta H_{+1} \cdot \left((I_{+1}/I_{-1})^{1/2} - 1 \right), \quad (3)$$

where $I_{\pm 1}$ are the amplitudes of the hyperfine structure (HFS) components $m = \pm 1$; $\Delta H_{\pm 1}$ is the peak-to-peak width of the low-field HFS component.

The correlation times of slow rotations of spin probes associated with colloidal sol particles were determined from the value of the residual anisotropy of the hyperfine interaction tensor by measuring the z-component of the tensor (A_{zz}), partially averaged due to molecular rotation, and the limiting value A_{zz}^L in the absence of molecular rotation at 77 K. Using the theory that treats the effects of slow Brownian rotation on the EPR spectra of nitroxyl radicals (see [17], chapter 3) and the obtained values of A_{zz} and A_{zz}^L, we determined the rotation correlation times for all points of the processing time dependence from the experimental dependences of A_{zz} on the processing time.

The hydrophobicity of the spin probe environment was characterized by the isotropic HFS constant on the nucleus N^{14} (a_{iso}) and the dimensionless parameter h [14]:

$$h(\text{THEOS}) = \frac{a(w) - a}{a(w) - a(THEOS)}, \quad (4)$$

where a, $a(w)$, $a(THEOS)$ are the a_{iso} values, respectively, in sol–gel, in water, in pure THEOS. In a polar environment (in water), the value of h is 0, in pure THEOS h (THEOS) is equal to 1. $a(w) = 16.75$ G, $a(THEOS) = 15.76$ G.

For the fast rotating regime that is realized for our narrow triplet EPR spectra, the a_{iso} (or h) values are well known to be correctly determined from the hyperfine splitting in the triplet EPR spectrum. The possible source of error in determining a_{iso} values in our case is the partial superposition of this triplet with the strongly immobilized EPR spectrum corresponding to species bound to sol or gel particles (see Fig. 4). However, as can be seen from Fig. 4, this superposition is noticeable for the central HFS components (I_0) and practically absent for the I_{+1} and I_{-1}
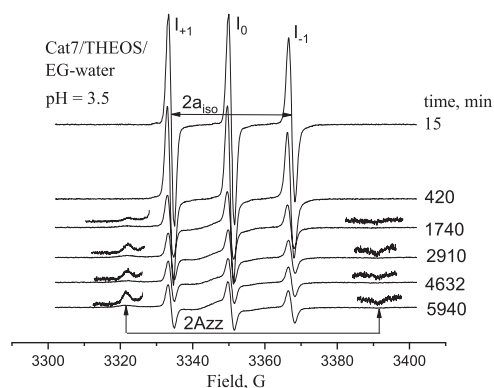
Fig. 4 ESR spectra of Cat7 in THEOS/EG-water sol–gel at different processing times after preparation. The initial concentrations of Cat 7, THEOS, and EG are 0.3, 0.72, and 0.54 M, respectively. The noisy outer spectral components correspond to the spin probes strongly immobilized on the sol/gel silica particles; pH 3.5

Fig. 5 Parameters of narrow triplet EPR signals of the Cat 7 probe in the liquid phase of the sol–gel system: the rotation correlation time τ_{eff} (light dots) and the amplitude of the HFS component $m = +1$ component (black dots) as a function of processing time. The initial composition is: Cat 7 (3×10^{-4} M), THEOS (0.73 M), EG (0.54 M); pH 3.5
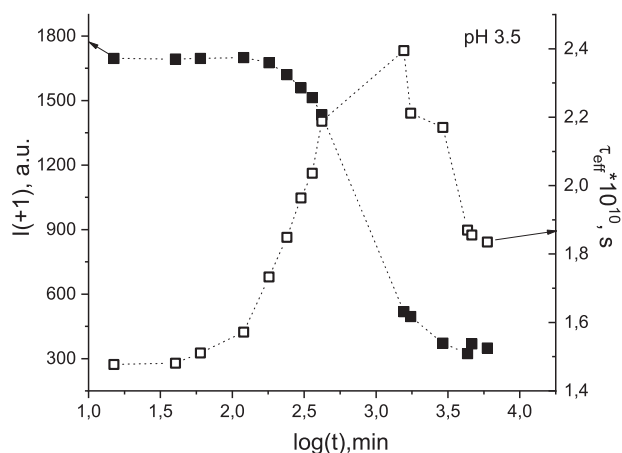
components. Therefore, in order to eliminate the possible error we determined the a_{iso} values by measuring these as a half distance between the I_{+1} and I_{-1} components. We performed also the spectral simulations for the model EPR spectra and found that the shift of the I_{+1} component due to the superposition for our experimental spectra does not exceed 0.03 G what corresponds to error in determining the h values less than 0.01.

The ratio of the number of probes in the liquid phase and probes adsorbed on the particle surface or pore walls was determined from the double integrals of the corresponding signals in the total EPR spectrum. The component $m = +1$ of the narrow signal is quite well resolved, although its intensity on the wings can be slightly distorted by the contribution from the spin probes giving strongly immobilized EPR spectrum (see Fig. 4). The double integral of this component multiplied by 3 (three HFS components of a narrow triplet signal) and divided by the double integral of the entire spectrum gives the relative fraction of probes in the liquid phase (P_f). The value $P_{imm} = (1 - P_f)$ determines the relative fraction of the strongly immobilized probes.

3 Results and discussion

The EPR spectra of Cat 7 in aqueous solution with THEOS and EG recorded in different processing times are shown in Fig. 4.

It can be seen that in the processing time interval of 15–10,000 min (log t 1–4) from the moment of preparation of the initial solution, two types of spin-labeled particles are formed, the EPR spectra of which indicate a change in the rotational mobility and concentration of these particles. Narrow symmetric triplet EPR spectra, characteristic of the

region of fast rotations, with rotation correlation times of ~10^{-10} s correspond to spin probes in solution; the concentration of these particles decreases over time. At processing times $t > 300$ min (log $t > 2.5$) from the moment of preparation, new spectral components (the outer noisy parts of them are marked by arrows) clearly appear and grow, corresponding to slow rotational diffusion of spin-labeled particles with rotation correlation times >10^{-7} s.

3.1 Narrow triplet EPR signals in the region of fast rotations

Figure 5 shows the kinetic dependences of the parameters of narrow triplet EPR signals of the Cat 7 probe: the correlation time of rotation, τ_{eff}, and the intensity of the component $m = +1$, I_{+1}. It can be seen that after a period of time log t ~2 (~100 min), the value of τ_{eff} begins to increase; after processing time of log t ~3.25 (1800 min), it passes through a maximum and falls in a time of ~3800 min.

Table 1 shows the isotropic splitting a_{iso} in the EPR spectra of Cat 7 probes in the liquid phase of the sol–gel system, as well as the polarity parameters h(THEOS) calculated from them (see the Experimental section).

From these data, it can be concluded that, despite the release of EG into the solution and a decrease in the water content during the hydrolysis of THEOS, the polarity of the probe environment in solution practically does not change and is close to the polarity of water.

In addition, for the neutral probe K6, the rotation correlation time, in contrast to Cat 7, changes in the sol–gel process by less than 7% and is close to the value of τ_{eff} in water. Obviously, the neutral probe K6 is practically not associated with sol particles and its rotational mobility

Table 1 Isotropic splittings a_{iso} in the EPR spectra of Cat 7 probes in the liquid phase of the sol-gel system and the polarity parameters h (THEOS) calculated from them

Time (min)	a_{iso} $(H_{-1} - H_{+1})/2$ (Gauss)	h(THEOS)
15	16.69	0.06
40	16.69	0.06
60	16.69	0.06
120	16.68	0.07
180	16.69	0.06
240	16.68	0.07
300	16.69	0.06
360	16.67	0.08
420	16.66	0.09
1560	16.63	0.12
1740	16.65	0.1
2910	16.67	0.08
4332	16.66	0.09
4632	16.67	0.08
5940	16.67	0.08

Fig. 6 Parameters of the broad EPR signals of the Cat 7 probe in the sol–gel phase of the system: the $2A_{zz}$ parameter (black dots) and τ_{imm}, the rotation correlation time of the strongly immobilized probes determined from the $2A_{zz}$ values (light dots) as a function of processing time. The initial composition is: Cat 7 (3×10^{-4} M), THEOS (0.73 M), EG (0.54 M); pH 3.5

reflects the viscosity of its environment in solution. This means that a significant increase in the value of τ_{eff} of the Cat 7 probe in solution is due not to a change in viscosity of the environment but most probably to a dynamic exchange between two states of the probe: (1) the free state in the solution, similar to the K6 probe and (2) the bound state on a sol particle, where the rotational mobility of the probe decreased sharply. The observed EPR spectrum and, accordingly, the increase in the observed rotation correlation time arise as a result of dynamic averaging between the two indicated states. An alternative explanation for the increase in the τ_{eff} due to a possible increase in viscosity during the formation of dimers, trimers, and sol particles in solution does not work, as noted above, since the EPR spectra of the neutral probe K6 do not show a corresponding change in the viscosity of the medium in which this probe is located. Models of the motion of the impurity molecules that are rather close to this one were proposed earlier on the base of NMR and EPR data in [3, 7, 8].

It can be seen that the onset of an increase in the value of τ_{eff} approximately coincides with the moment of appearance and growth of a strongly immobilized EPR signal, which apparently belongs to probes bound to the sol particles. Therefore, one might think that an increase in τ_{eff} for probes in solution is due to chemical exchange between them and the probes responsible for strongly immobilized EPR spectra. However, a comparison of the behavior of both EPR signals at longer processing times shows that the value of τ_{eff} decreases in the time range log t ~3–4, while the strongly immobilized probes continue to grow (see Figs. 5–7),
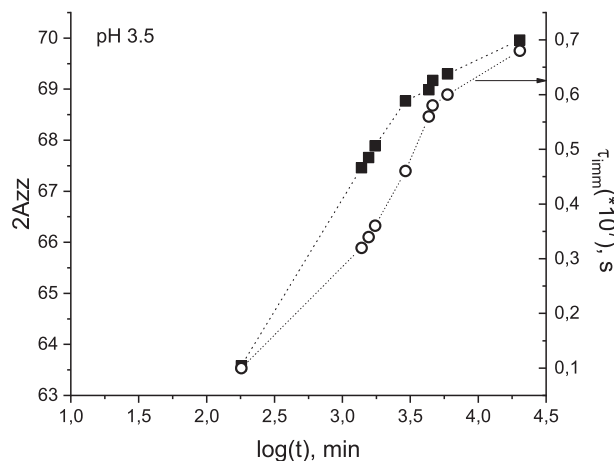
i.e., there is no correlation between changes in the parameters τ_{eff} of free probes in solution and changes in the concentrations of probes responsible for strongly immobilized EPR spectra. The existence of a correlation at the initial stage of kinetics and its absence at the stage of decreasing τ_{eff} is most probably due to the fact that there are two types of probe binding sites on sol particles: (1) weakly bound sites, apparently on the surface of sol particles, where the probes rapidly dissociate into solution and bind again to the sol particles; in this case, due to the short lifetime of such probes on the particle surface, only the EPR spectrum dynamically averaged over these two states is observed; and (2) sites with a strong bond, apparently, in the particles volume, where the lifetime of the probe is long enough (i.e., it should be much longer than the inverse difference between the resonance frequencies in the free and bound states).

What is the cause for the drop in τ_{eff} (see Fig. 5)? The fall began when the volume fraction of the sol and the size of the particles were still increasing. There is not only a decrease in τ_{eff}, but also a decrease in the concentration of free probes. The latter decrease is apparently due to the above-mentioned sorption of positively charged Cat 7 probes on sol particles having a negative potential. In terms of the onset time, these events correlate with the formation and growth of sol particles (see Figs. 5 and 6). The decrease in τ_{eff} is apparently also due to the aggregation of sol particles forming a quasi-solid (or gel) phase, which leads to a decrease in the exchange rate due to obstacles, created by the gel particles. A more significant reason for the drop in τ_{eff} is a decrease in the surface compared to the total surface of sol particles due to the formation of bulk aggregates from

sol particles. Figure 6 shows the kinetics of changes in the parameters of the EPR spectra of probes bound to sol particles, which are responsible for the strongly immobilized EPR spectra.

The parameter $2A_{zz}$ in the EPR spectrum (see Fig. 5) characterizes the rotational mobility of a strongly immobilized spin probe adsorbed on a sol or gel particle. The quantity $2A_{zz}$ is the doubled z-component of the HFS tensor, partially averaged due to rotational motion. The correlation time of this motion can be estimated if, in addition to the value $2A_{zz}$, its limiting value in the absence of rotation ($2A_{zz}^{L}$) is known and the model of isotropic rotation is used. To determine the $2A_{zz}^{L}$ values, we measured the EPR spectra of the sol–gel samples at 77 K. Using the EPR theory for slow Brownian rotation [17], we determined the rotation correlation times (τ_{imm}) using the $2A_{zz}$ and $2A_{zz}^{L}$ values for all points of the time dependence. These correlation times, as can be seen from Fig. 6, lie in the sub-microsecond range and increase with the evolution time of the sol–gel system. Assuming further that the quantities refer to probes rigidly immobilized on the surface of the sol or gel particles, it is possible to estimate the sizes of the sol particles themselves in the approximation of their spherical shape using the Stokes–Einstein equation:

$$\tau_{imm} = \eta V/kT, \tag{5}$$

where η is the microviscosity of the probe environment in solution, V is the hydrodynamic volume of a sol particle. The magnitude of microviscosity was taken to correspond to the aqueous environment, since the values of the accompanying polarity parameters of the environment, a_{iso} and h(THEOS), practically did not change during the reaction (see Table 1) and corresponded to an almost aqueous environment.

Figure 7 shows that the Stokes radii of particles increase in the range of several nm during the sol–gel process and do not reach a plateau. It should be noted that the model of free
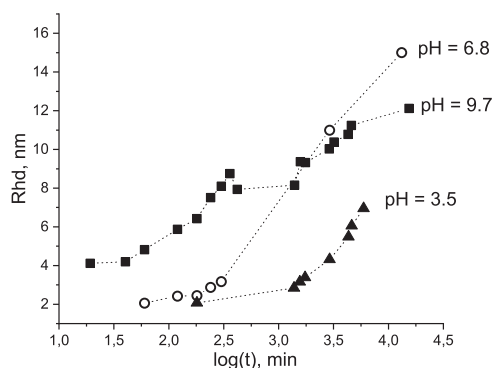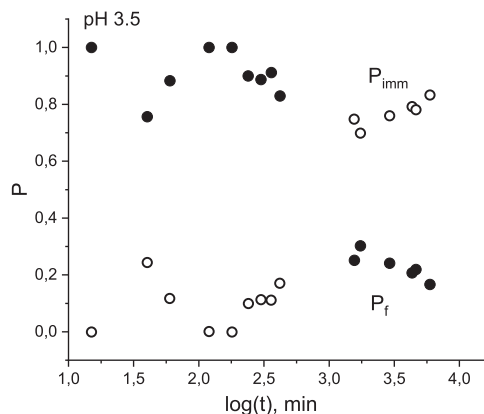
Brownian rotation used here is suitable for sol particles in a liquid solution but provides only qualitative description for suspensions of gel particles, when there is an interaction between the particles. (This issue requires further investigation).

Furthermore, important parameters of a heterogeneous sol–gel system, which were obtained from the analysis of EPR spectra, are the relative fractions of probes in the liquid phase (P_f) and probes bound to the particles (P_{imm}) were calculated from the total EPR spectra as described in the Experimental section. The dependences of these parameters on the processing time of the sol–gel process for different pH values are given in Figs. 8, 11, and 14.

Figure 8 shows that up to the time log (t) min ~2.0 after sample preparation, the proportion of the immobilized probes, taking into account the experimental scatter, is equal to zero, and the contribution from the normalized narrow triplet is, respectively, equal to unity. After a time log (t) min ~2.1, a spectrum appears from the spin probes immobilized on the sol particles, its contribution increases, while the contribution from the narrow triplet decreases. After log (t) min ~3.0, the contributions of both signals become equal, and then the proportion of free probes tends to 20%, while the proportion of immobilized probes tends to 80%.

It is of some interest to what extent it can be corrected to estimate the relative fractions of two phases, a liquid solution, and sol or gel particles by using the relative proportions of spin probes in both phases. In reality, the EPR of weakly and strongly immobilized signals determines the ratio of the fractions of these signals, rather than the fractions of monomers and sol particles. To test the correctness of this approach, we used another nitroxide radical, Cat 14, in which instead of the heptyl group there is a longer myristyl group bound to the quaternary nitrogen atom. Our experiments have shown that the fraction of the immobilized signal at all times increases as compared to Cat 7, which is naturally explained by the more hydrophobic

Fig. 7 Hydrodynamic radii R_{hd} of sol particles in the sol/gel system as functions of the processing time at pH: 3.5, 6.8, 9.7. The initial composition is: Cat 7 (3×10^{-4} M), THEOS (0.73 M), EG (0.54 M); pH 3.5, 6.8, 9.7

Fig. 8 Integral contributions to the EPR signal from free probes (P_f, black dots) and from probes immobilized on sol–gel particles (P_{imm}, light dots) as a function of processing time, pH 3.5

nature of the Cat 14. However, the fraction of immobilized EPR signals also increases with an increase in the fraction of the sol–gel phase due to an increase in the interphase surface at which the probes can be bound. This means that with the help of the same probe, it is possible to monitor the changes in the proportions of both phases during the sol–gel transformation, changes in the composition of the system, pH, and temperature.

3.2 pH dependence of the parameters of spin probes during the sol–gel process

A significant number of works have been devoted to the study of the effect of pH on the chemical stages of sol–gel processes—the reactions of hydrolysis and polymerization (see reviews in [1, 2]). Iler [1] divides the polymerization process into approximately three pH ranges: <2; 2–7; >7. The points of zero charge of the sol particles and the iso-electric point (where the mobility of the particles is zero) are in the range of pH 1–3. pH 7 is the limit, since the solubility of the particles and the dissolution rates are maximum around or at pH 7. In addition, since the growing particles are highly ionized above pH 7, their growth occurs without aggregation and gelation. In view of the widespread use of sol–gel materials as matrixes for the functional molecules in photonics and sensor systems, it seemed important to study the effect of pH on the distribution of spin probes in a heterogeneous sol–gel system and the molecular dynamics of probes at various stages of sol–gel processes.

Therefore, along with the data for pH 3.5, we investigated changes in the parameters of spin probes in the sol–gel process at pH in the neutral and alkaline regions. The results obtained with the Cat 7 probe are shown for pH
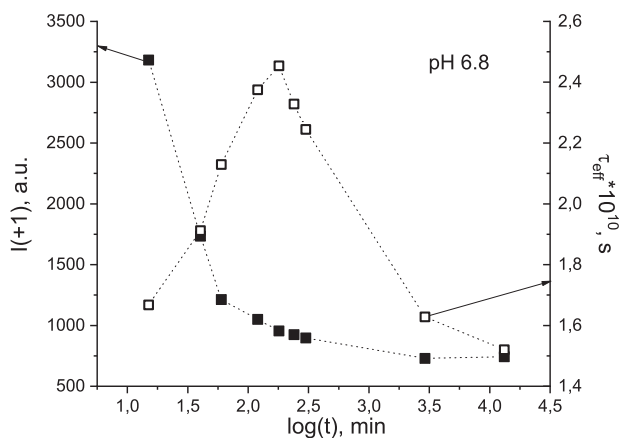
3.5 in Figs. 5–8, for pH 6.8 in Figs. 9–11, and for pH 9.7 in Figs. 12–14.

As can be seen from the presented figures, the parameters of molecular dynamics and the partition of positively charged nitroxyl probes turned out to be very sensitive to changes in pH. Changes in pH obviously affect the rates of reactions involved in sol–gel processes (see Eqs. (1) and (2)), which leads to a change in the composition of the reaction mixture and, accordingly, to a change in the designated parameters of Cat 7 probes, which do not depend on pH in simple solvents. From the data in the figures, the following main differences in the kinetics of sol–gel processes at different pH can be identified: (1) the drop in the intensity of narrow triplet signals from probes in solution at pH 6.8 and 9.7 occurs much earlier than for pH 3.5: 80 min for pH 3.5;
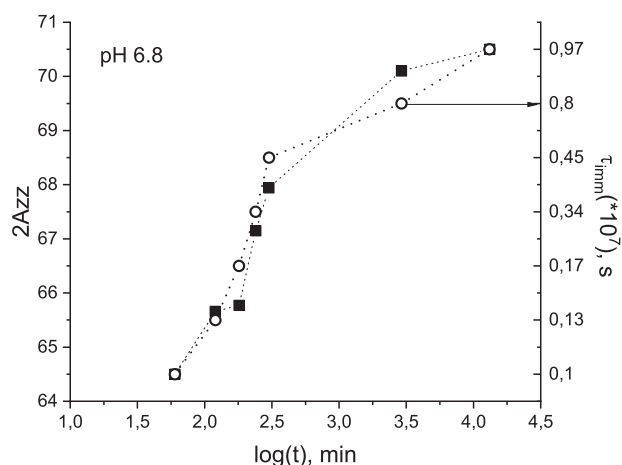
Fig. 10 Parameters of the broad EPR signals of the Cat 7 probe in the sol–gel phase of the system: the $2A_{zz}$ parameter (black dots) and τ_{imm}, the rotation correlation time of the strongly immobilized probes determined from the $2A_{zz}$ values (light dots) as a function of processing time. The initial composition is: Cat 7 (3×10^{-4} M), THEOS (0.73 M), EG (0.54 M); pH 6.8
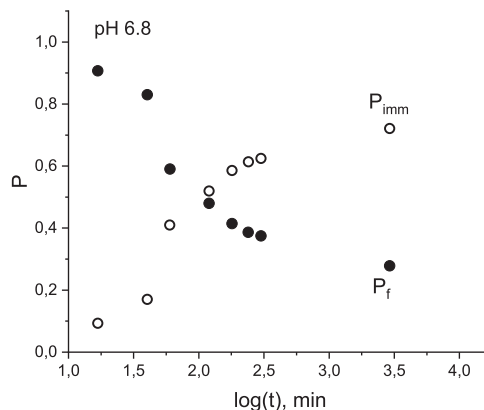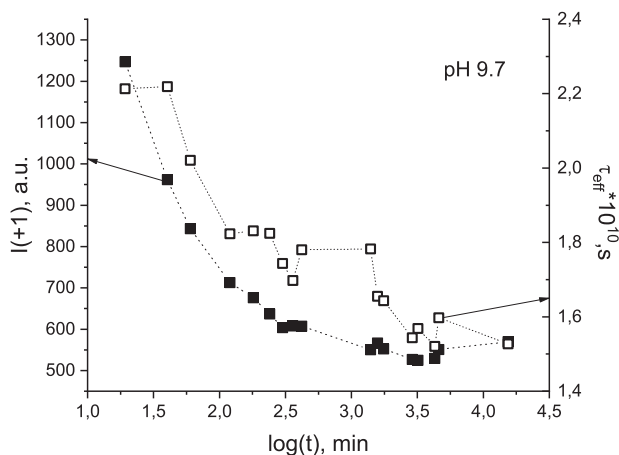
Fig. 9 Parameters of narrow triplet EPR signals of the Cat 7 probe in the liquid phase of the sol–gel system: the rotation correlation time τ_{eff} (light dots) and the amplitude of the HFS $m = +1$ component (black dots) as a function of processing time. The initial composition: Cat 7 (3×10^{-4} M), THEOS (0.73 M), EG (0.54 M), pH 6.8

Fig. 11 Integral contributions to the EPR signal from free probes (P_f, black dots) and from probes immobilized on sol–gel particles (P_{imm}, light dots) as a function of processing time, pH 6.8

Fig. 12 Parameters of narrow triplet EPR signals of the Cat 7 probe in the liquid phase of the sol–gel system: the rotation correlation time τ_{eff} (light dots) and the amplitude of the HFS $m = +1$ component (black dots) as a function of processing time. The initial composition: Cat 7 $(3 \times 10^{-4}$ M), THEOS (0.73 M), EG (0.54 M), pH 9.7
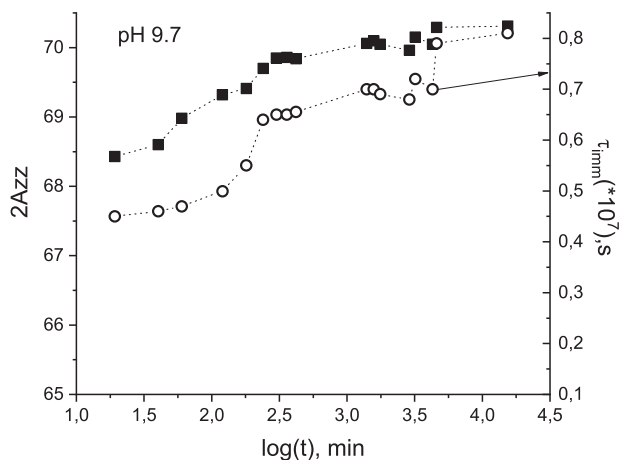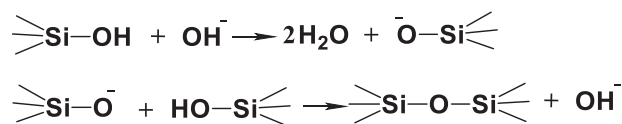

Fig. 13 Parameters of the broad EPR signals of the Cat 7 probe in the sol–gel phase of the system: the $2A_{zz}$ parameter (black dots) and τ_{imm}, the rotation correlation time of the strongly immobilized probes determined from the $2A_{zz}$ values (light dots) as a function of processing time. The initial composition is: Cat 7 $(3 \times 10^{-4}$ M), THEOS (0.73 M), EG (0.54 M); pH 9.7

~20 min for pH 6.8; and shorter than 10 min for pH 9.7. (2) An increase in the correlation time of rotation of Cat 7 probes in the THEOS solution due to the dynamic exchange between the free states of the probes in the solution and the binding sites on the surface of colloidal sol particles at pH 6.8 begins in 30 min after mixing and reaches a maximum in 90 min earlier than for pH 3.5, at which these times are equal to 90 min and 30 h, respectively. At pH 9.7, the increase in time to the process of kinetics (see Table 1) and corresponded to the aqueous environment τ_{eff} and reaching the maximum occur in a time shorter than the spectrum registration time, as a result of which only the decay curve τ_{eff} can be observed. (3) The appearance of a strongly immobilized
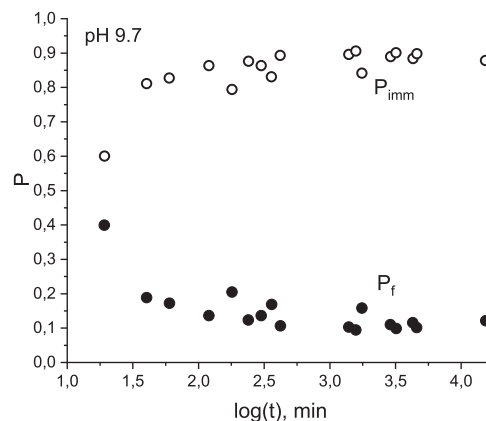
Fig. 14 Proportions to the EPR signal from free probes (P_f, black dots) and from probes, immobilized on sol–gel particles (P_{imm}, light dots) as a function of processing time. The initial composition is: Cat 7 $(3 \times 10^{-4}$ M), THEOS (0.73 M), EG (0.54 M); pH 9.7

signal from the bound probes at pH > 7. These differences are obviously due to the pH dependence of the main reactions occurring in the sol–gel process of hydrolysis and condensation (Eqs. (1) and (2)). Polymerization at pH 3.5 and higher pH also occurs according to equations:

$$\equiv\!Si\!-\!OH \ + \ OH^- \longrightarrow 2H_2O \ + \ ^-O\!-\!Si\!\!\equiv$$

$$\equiv\!Si\!-\!O^- \ + \ HO\!-\!Si\!\!\equiv \ \longrightarrow \ \equiv\!Si\!-\!O\!-\!Si\!\!\equiv \ + \ OH^-$$

Since condensed particles at pH > 6.8 are mostly ionized and therefore repel each other, particle growth occurs predominantly through the addition of monomers to the condensed particles rather than through the aggregation of charged particles. Particles with a diameter of 1–2 nm are formed within a few minutes at pH 6.8 and 9.7. Due to the dependence of solubility on particle size, the growth of primary particles occurs according to the mechanism of Oswald ripening [1]. Since growth occurs by dissolving small particles and their deposition on large particles, the growth rate depends on the particle size distribution, which can be seen from different time dependences of the average Stokes radii of sol particles at different pH (Fig. 8). In the absence of salts, no chain formation or aggregation occurs because at high pH the particles repel each other.

4 Conclusion

It is shown in this work that the use of spin probes allows one to obtain important information on the behavior and properties of impurity probe molecules in a sol–gel matrix during its processing time. In contrast to complexes of paramagnetic ions of the VO^{2+} or Gd^{3+} type, changes in the spectral characteristics of nitroxide probes can be

reliably associated with changes in important structural and dynamic parameters of the probes—their partition in a heterogeneous sol–gel system and molecular dynamics.

In the course of this processing, the mutual influence and interdependence of various parameters of a sol–gel system containing impurity molecules is revealed. Thus, the concentration of "free" probes in solution is influenced by the time-dependent (transient) adsorption of probes on the growing surfaces of sol particles

Two types of sorption of impurity molecules on colloidal sol particles were found, due to the binding of probes to the surface and, apparently, to binding sites in the bulk of colloidal particles.

The effective rotation correlation time (τ_{eff}) characterizes the fast dynamic exchange with the growing surface of the sol particles. The value of τ_{eff} increases due to the fact that this surface increases with the addition of monomers to colloidal sol particles.

The value of τ_{eff} further decreases apparently due to the fact that the free surface of the sol–gel particles decreases as a result of aggregation. At the same time, according to the EPR spectra, the concentration of free probes in the solution decreases symbatically.

The probes, which correspond to the immobilized EPR spectra, do not exchange or exchange slowly with the probes in solution. With an increase in the processing time, the concentration of these probes increases, and their rotational mobility decreases due to an increase in the size of these particles. Measurement of the rotational correlation times of the probes associated with the colloidal particles of the probes made it possible to estimate the sizes of these particles.

Thus, the use of spin probes made it possible, first, to obtain information on the behavior and properties of impurity probe molecules in a sol–gel silica gel matrix during its processing time. Second, in the course of this evolution, the mutual influence and interdependence of various parameters of a sol–gel system containing impurity functional molecules is revealed. Thus, the concentration of "free" probes is influenced by the time-dependent adsorption of the probes on growing sol particles; the effective correlation time of rotation of "free" probes is determined by the dynamic exchange of these probes with the surface of growing particles, which changes with time in the sol–gel process.

The limitation of this research is the use of relatively narrow set of spin probes. Although some regularities found in this study: the existence of the effective rotational correlation time for the spin probes in solution and its variation with the processing time, composition and pH of the S/G medium, apparently present a general interest, it would be interesting to uncover similar or different regularities for chemically different spin probes. Also, of special interest can be hybrid spin and fluorescent probes that would give combined information on dynamical structure and optical parameters of the S/G systems.

Data availability

Data and material can be obtained from the corresponding author on demand.

Compliance with ethical standards

Conflict of interest The authors declare no competing interests.

Publisher's note Springer Nature remains neutral with regard to jurisdictional claims in published maps and institutional affiliations.

References

1. Iler RK (1979) The chemistry of silica. Wiley, New York
2. Brinker CJ, Scherer GW (1990) Sol-gel science. The physics and chemistry of sol-gel processing. Academic Press
3. Liu G, Li Y, Jonas J (1991) Confined geometry effects on reorientational dynamics of molecular liquids in porous silica glasses. J Chem Phys 95:6892–6901
4. Shames A, Lev O, Iosefzon-Kuyavskaya B (1994) In situ EPR study of sol-gel processes. J Non-Cryst Solids 175:14–20
5. Dunn B, Zink JI (1997) Probes of pore environment and molecule–matrix interactions in sol–gel materials. Chem Mater 9 (11):2280–2291
6. Matsui K, Kaneko T, Yaginuma Y, Ryu M (1997) ESR study of a nitroxide radical in sol-gel glasses. J Sol-Gel Sci Technol 9:273–277
7. Wonorahardjo S, Ball G, Hook J, Moran G (1998) NMR relaxation studies of porous sol-gel glasses. Magn Reson Imaging 16(5-6):511–513
8. Wheeler KE, Lees NS, Gurbiel RJ, Hatch SL, Nocek JM, Hoffman BM (2004) Electrostatic influence on rotational mobilities of sol–gel-encapsulated solutes by NMR and EPR spectroscopies. J Am Chem Soc 126(41):13459–13463
9. Shchipunov YA, Karpenko TY, Krekoten AV, Postnova IV (2005) Gelling of otherwise nongelable polysaccharides. J Colloid Interface Sci 287(2):373–378
10. Brandhuber D, Torma V, Raab C, Peterlik H, Kulak A, Hüsing N (2005) Glycol-modified silanes in the synthesis of mesoscopically organized silica monoliths with hierarchical porosity. Chem Mater 17(16):4262–4271
11. Koshkin AV, Aleksandrova NA, Ivanov DA (2017) The fluorescence study of a styryl dye supramolecular complexes with cucurbit[6]uril and cucurbit[7]uril included in gels. J Sol-Gel Sci Technol 81(1):303–310
12. Mazur M, Husarikova L, Rhodes CJ, Valko M (2015) Tetraethyl orthosilicate (TEOS)-based sol–gel process monitored by EPR spectroscopy with VO(II) cations as a spin-probe. J Sol-Gel Sci Technol 76(1):110–119
13. Mazur M, Poprac P, Valko M, Rhodes CJ (2016) 'U-spectrum' type of Gd(III) EPR spectra recorded at various stages of TEOS-based sol–gel process. J Sol-Gel Sci Technol 79:220–227

14. Livshits VA, Demisheva IV, Meshkov BB, Tsybyshev VP, Alfimov MV (2009) A study of adsorption and molecular dynamics of spin-labeled molecules on the surface of silica nanoparticles. Nanotechnologies Russ 4:45–54. https://link.springer.com/content/pdf/10.1134/S1995078009010054.pdf

15. Ionova IV, Alfimov MV, Livshits VA (2011) Adsorption and molecular dynamics of spin probes on hydrophobizated silica gel microparticles: EPR spin-label study. Nanotechnologies Russ 6:88–95. https://link.springer.com/content/pdf/10.1134/S1995078011010071.pdf

16. Ionova IV, Voronina LV, Meshkov BB, Alfimov MV, Livshits VA (2013) Complexation of a gaseous spin probe with cyclodextrins bound to the silica microspheres: Molecular dynamics of the complexed probes and the effect of aromatic hydrocarbon vapors on it. Nanotechnologies Russ 8:592–602

17. Berliner LJ (1976) Spin labeling. Theory and applications. Biological magnetic resonance, Chapter 3. Plenum Press, New York

18. Wasserman AM, Kovarsky AL (1986) Spin labels and probes in physical chemistry of polymers. Science, Moscow (in Russian)